Martin Horcajo, S., Pomeroy, J. W., Lambert, B., Jung, H., Blanck, H., & Kuball, M. (2016). Transient thermoreflectance for device temperature assessment in pulsed-operated GaN-based HEMTs. In CS MANTECH 2016: International Conference on Compound Semiconductor Manufacturing Technology. (pp. 283-286). CS Mantech.

Peer reviewed version

Transient Thermoreflectance for Device Temperature Assessment in Pulsed-Operated GaN-based HEMTs

Sara Martin-Horcajo[1], James W. Pomeroy[1], Benoit Lambert[2], Helmut Jung[3], Herve Blanck[3], and Martin Kuball[1]

[1]Centre for Device Thermography and Reliability (CDTR), University of Bristol, Tyndall Avenue, Bristol BS8 1TL, United Kingdom
[2]United Monolithic Semiconductors SAS, Orsay, France
[3]United Monolithic Semiconductors GmbH, Wilhelm-Runge-Str, 11, 89081 Ulm, Germany
e-mail: **sara.martinhorcajo@bristol.ac.uk** Phone: +44 117 331 8110

Keywords: HEMT, GaN, self-heating, transient thermoreflectance, time-resolved Raman, thermal modelling

Abstract

Transient thermoreflectance measurements were demonstrated as a reliable technique for the thermal assessment of pulsed-operated HEMTs. Thermal modeling and time-resolved micro-Raman thermography were used for the determination of thermoreflectance coefficients of the metal contacts under study. The need of the extraction of the thermoreflectance coefficient value for each metal present at the device was demonstrated.

INTRODUCTION

GaN-based HEMTs have been developed in order to meet the requirements of enhanced RF power applications [1]. This extensive research has resulted in substantial performance improvements such as an increase of the output power densities up to 30-40 W/mm [1], although reliable device operation typically only uses up to 7 W/mm. These high power density levels lead to significant self-heating, which not only decreases the device performance but also affects the device reliability. Therefore, knowing the temperature under operating conditions is important for the optimization of both device design and reliability [2, 3]. A number of numerical and experimental approaches have been proposed for the evaluation of the device temperature, such as 3D finite element (FE) simulations [4], electrical measurement techniques [3, 5], micro-Raman spectroscopy [2], IR-thermography [6], scanning thermal microscopy [7], and thermoreflectance imaging [8]. However, only few methods have been developed for the thermal assessment of pulsed-operated HEMTs [9].

In this contribution, we demonstrate transient thermo-reflectance measurements as a potentially accurate and fast technique to obtain the temperature profiles at different locations in the GaN-based HEMTs under pulsed operation conditions. To do so, we have also performed time-resolved micro-Raman thermography measurements and FE simulations to extract the thermoreflectance coefficients.

EXPERIMENTAL DETAILS

Thermoreflectance is an optical, non-contact technique which correlates the temperature change (ΔT) of a material with the temperature-induced optical reflectivity variation (ΔR). This relation can be defined as [10]:

$$\frac{\Delta R}{R} = K \cdot \Delta T \qquad (1)$$

where R is the mean optical reflectivity, and K is the thermoreflectance coefficient which is dependent on the material, and on the light wavelength [10, 11]. This technique has been widely used as a tool for the measurement of thermal properties of materials, such as for the assessment of the interfacial thermal resistance of as-grown GaN-on-diamond wafers [12]. Although it has been also applied on HEMTs for their thermal assessment [13], its use has been limited by the need of the extraction of the thermoreflectance coefficients. This task can be challenging since they depend not only on the material but also on the passivation layer equally present [14].

A 532 nm CW laser (2nd harmonic of Nd:YAG) was used as a probe beam to monitor the reflectivity change in the time domain. A Leica 50x, NA=0.60 objective lens was used to focus the laser beam spot onto the metal diameter of ~0.5-0.6 µm. A beam splitter was used to sample the reflected beam intensity which was recorded using a 200 MHz bandwidth silicon photodiode and transimpedence amplifier connected to an Agilent DSO-X 3034A digital oscilloscope; each measurement takes approximately 2 minutes. The dominant reflection occurs at the passivation layer/metal interface due to their greatest refractive index contrast, which makes the measurements most sensitive to the temperature variation at the surface of the metal under study. It is worth to mention that we verified that there is a reasonable good linear relationship between the refractive change and the surface temperature variation; the probe laser wavelength was chosen for this reason away from the local maximum or minimum of the reflectance spectrum [15].

The devices used in this study were AlGaN/GaN/SiC HEMTs (Figure 1). They consisted of 100 µm-wide single-finger, 0.5 µm long T-gate, 1.5 µm gate-source spacing, and

4 µm gate-drain gap. V_{GS} was pulsed from -3 V (below its threshold voltage) to 0 V with a period of 10 µs and 25 µs, and a 55% duty cycle, while a constant DC voltage (from 25 V to 50 V) was applied to the drain. Thermoreflectance measurements were performed at different locations in pulsed-operated devices (see Figure 1).

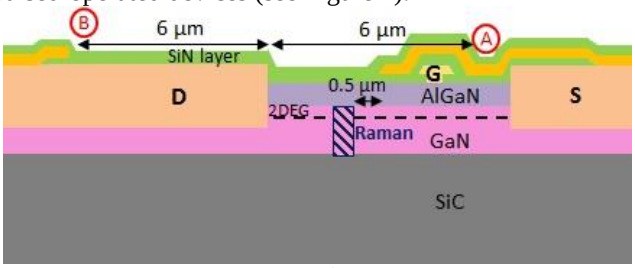

Figure 1. Schematic cross-section of the studied AlGaN/GaN-on-SiC HEMT, showing the area in the GaN layer measured by Raman thermography. Position A and B correspond to the locations where thermoreflectance measurements were carried out at the source field plate and drain contact surfaces, respectively.

Experimental Results And Discussion

In order to determine from $\Delta R/R$ the actual temperature, thermoreflectance coefficients are needed for the specific locations measured on the devices. In the literature, the most common procedure for the extraction of K values consists of placing the device in a temperature controlled external heater or in a Peltier cell and recording the change in reflectivity while the temperature is measured simultaneously using a thermocouple [16]. However, this calibration process may present some drawbacks, for instance, the stage can move during the heating process introducing some error in the measurement of the reflectivity, when small device structures are considered, as well as reflectivity changes can be small in the 10^{-3} to 10^{-4} range. Moreover, the thermocouple may not provide accurately the temperature in the location of interest due to the thermal contact resistance [17].

In this work, we have used a different calibration process to extract the K value for the metals present at the device. It involves both time-resolved micro-Raman spectroscopy measurements [9] and FE thermal simulations using ANSYS. Thermal conductivity parameters of 160 W/m·K ($T^{-1.4}$ temperature dependence) for GaN, thermal conductivity of 440 W/m·K ($T^{-1.1}$ temperature dependence) for SiC, and 1 W/mK for the passivation layer were used for the simulations, similar to our previous work [18]. Firstly, we have measured using micro-Raman the average GaN temperature at 0.5 µm from the source field plate end in a pulsed-operated device with a period of 10 µs and 50% as duty cycle. Secondly, we have compared the obtained temperature profiles with the simulations to validate the thermal model. Figure 2 shows the good agreement between experiment and simulation. Then, the ΔT simulations were correlated with the $(-1)\cdot\Delta R/R$ profiles measured at the source field plate (Figure 3); the need of multiplying the $\Delta R/R$ signal by (-1) indicates that the K of the source field plate metal has a negative value for 532 nm; taking into account eq. 1, we have extracted its value $(-8.7\cdot10^{-4} \pm 0.2\cdot10^{-4})$ C^{-1} as the linear fit slope of $(-1)\cdot\Delta R/R$ signal versus simulated ΔT (see inset of Figure 3).

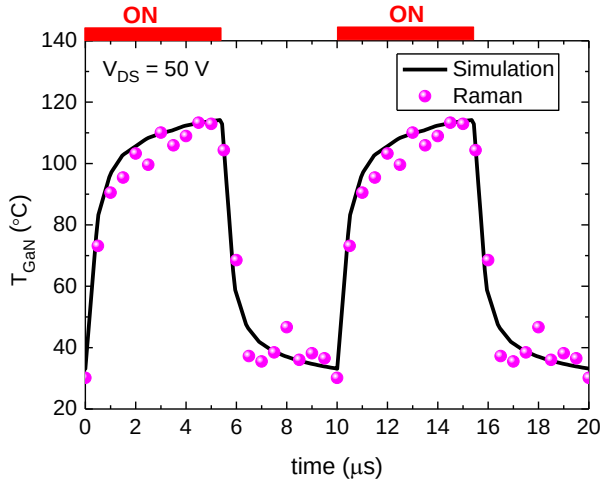

Figure 2. Raman thermography determined device temperature (average temperature of the GaN) at 0.5 µm away from the source field plate end, towards the drain contact side, and comparison to simulated temperature.

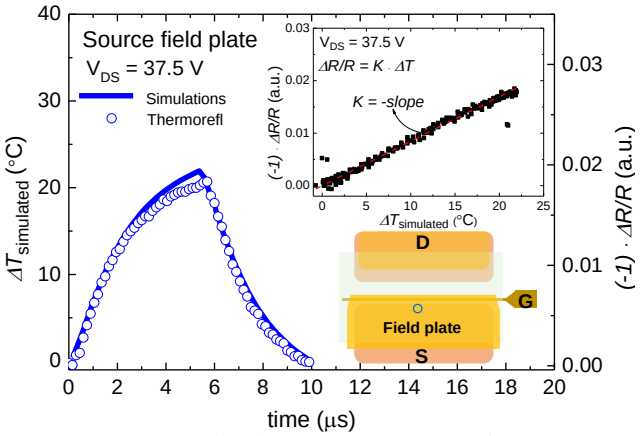

Figure 3. Correlation of $\Delta R/R$ determined by thermoreflectance in the source field plate (location A in Figure 1), 6 µm away from the drain contact edge, with ΔT simulated values for V_{DS} = 37.5 V. The extraction of K value is shown as an inset. The top-view schematic illustrates where the thermoreflectance measurements were performed.

Similarly, the ΔT simulations were correlated with the $\Delta R/R$ profiles measured at the drain contact (Figure 4); and taking into account eq. 1, the K value of the drain contact was also extracted: $(9.4\cdot10^{-4} \pm 0.5\cdot10^{-4})$ C^{-1} (see inset of Figure 4). Interestingly, it has different sign and value than the K of the source field plate metal, which can be attributed to the contact's different composition, and roughness. Therefore, in contrast with what was proposed by Maize *et al.* [16], the thermal mapping may require the calibration of the K value for each metal, to enable accurate temperature determination.

Finally, using the extracted K values, we have obtained the temperature profiles at different locations along the source field plate and the drain contact while the device

operates under different pulsed conditions (Figure 5). It is worth to mention that we have also attempted to evaluate the temperature at the semiconductor surface in the gate-drain gap but the results were not consistent, probably due to the contribution of the sub-surface reflections to the total reflectance [15].

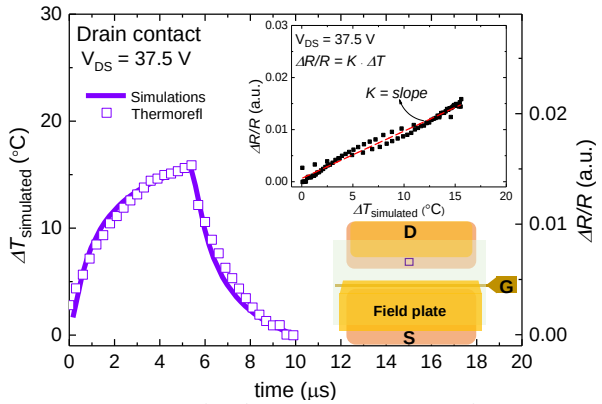

Figure 4. Correlation of $\Delta R/R$ determined by thermoreflectance in the drain contact (location B in Figure 1), 6 µm from the drain contact edge, with ΔT simulated values for V_{DS} = 37.5 V. The extraction of K value is shown as an inset. The top-view schematic illustrates where the thermoreflectance measurements were performed.

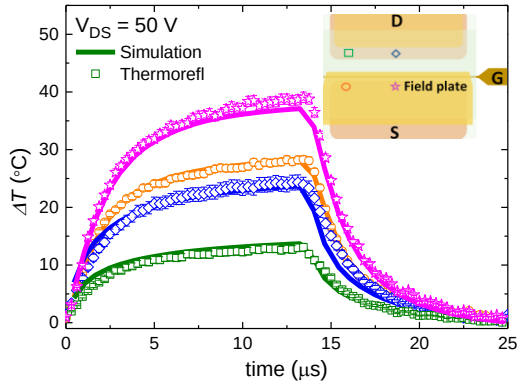

Figure 5. Thermoreflectance determined ΔT profiles at different locations in the device (shown in the inset). Simulated values are also included for comparison.

Similar to time resolved micro-Raman, thermoreflectance measurements exhibit a good temporal resolution and a good spatial resolution (~0.5-1.0 µm). However, these measurements are faster to perform once the thermoreflectance coefficients have been determined. Thermoreflectance measurements provide the temperature at the metal surface, whereas micro-Raman spectroscopy provides the average temperature of the GaN device layer. Thus, micro-Raman can enable the temperature assessment near the location of the maximum temperature when the device design does not include any field-plate. In combination with thermoreflectance measurements of the metal contacts, when combined with simulation this enables improved accuracy for the determination of device temperature. From an industrial point of view, this technique may exhibit benefits as it is fast and does not require sophisticated equipment, as long as knowledge of the metal contact temperature is sufficient. Regarding the calibration of thermoreflectance coefficients, their values should be valid from device to device since they would be fabricated following a well-stablished and reproducible processing.

CONCLUSIONS

We have demonstrated thermoreflectance measurements as a reliable technique to evaluate the self-heating in pulsed-operated HEMTs. The need to determine accurately the thermoreflectance coefficients of the metal contacts of HEMTs was demonstrated, which can be a limiting factor of this technique if their values are not extracted accurately. We have proposed a new procedure for their calibration which is less prone to uncertainties. The combination of both Raman thermography and thermoreflectance measurements can enable an extensive thermal characterization of device in operation.

ACKNOWLEDGEMENTS

This work was supported by E2coGaN, and MCM ITP Extreme GaN projects. The authors would like to thank THALES Optronics and both governmental agencies, DSTL and DGA for their technical and financial supports as well as all our partners for their deep involvement in these collaborative research projects. We also acknowledge funding from the Engineering and Physical Sciences Research Council (EPSRC) under EP/L007010/1.

REFERENCES

[1] U. K. Mishra, L. Shen, T. E. Kazior, and Y. F. Wu, in Proc. *IEEE*, **96(2)**, 287 (2008).

[2] M. Kuball, J. M. Hayer, M. J. Uren, T. Martin, J. C. H. Birbeck, R. S. Balmer, and B. T. Hughes, *IEEE Electron Device Lett.*, **23(1)**, 7 (2002).

[3] R. J. T. Simms, J. W. Pomeroy, M. J. Uren, T. Martin, and M. Kuball, *IEEE Trans. Electron Devices*, **55(2)**, 478 (2008).

[4] F. Bertoulzza, N. Delmonte, and R Menozzi, *Microelectron. Reliab.*, **(49)5**, 468 (2009).

[5] S. Martin-Horcajo, A. Wang, M.-F. Romero, M. J. Tadjer, and F. Calle, *IEEE Trans. Electron Devices*, **(60)10**, 4105 (2013).

[6] A. Sarua, H. Ji, M. Kuball, M. J. Uren, T. Martin, K. P. Hilton, and R. S. Balmer, *IEEE Trans. Electron Devices*, **(53)10**, 2438 (2006).

[7] R. Aubry, J.-C- Jacquet, J. Weaver, O. Durand, P. Dobson, G. Mills, M.-A. di Forte-Poisson, S. Cassette, and S.-L. Delage, *IEEE Trans. Electron Devices*, **(54)3**, 385 (2007).

[8] K. Maize, G. Pavlidis, E. Heller, L. Yates, D. Kending, S. Graham, and Ali Shakouri, in Proc. *CSICs Symposium*, 2014.

[9] M. Kuball, G. J. Riedel, J. W. Pomeroy, A. Saura, M. J. Uren, T. Martin, K. P. Hilton, J. O. Maclean, and D. J. Wallis, *IEEE Electron Device Lett.*, **(28)2**, 86 (2007).

[10] S. Dilhaire, S. Grauby, and W. Claeys, *Appl. Phys. Lett.*, **(84)5**, 822 (2004).

[11] G. Tessier, S. Hole, and D. Fournier, *Appl. Phys. Lett.*, **(78)16**, 2267 (2001).

[12] H. Sun, J. W. Pomeroy, R. B. Simon, D. Francis, F. Faili, D. J. Twitchen, and M. Kuball, in Proc. *CS-Mantech Conference*, 151 (2015).

[13] K. Maize, E. Heller, D. Dorsey, and A. Shakouri, in Proc. *IEEE SEMI-THERM Symposium*, 173 (2012).

[14] P. L. Komarov, M. G. Burzo, and P. E. Raad, in Proc. THERMINIC, 17 (2007).

[15] H. Sun, J. W. Pomeroy, R. B. Simon, D. Francis, F. Faili, D. J. Twitchen, and M. Kuball, in Proc. *CS-Mantech Conference*, 151 (2015).

[16] K. Maize, E. Heller, D. Dorsey, and A. Shakouri, in Proc. *IEEE SEMI-THERM Symposium*, 173 (2012).

[17] T. Favaloro, J. H. Bahk, and A. Shakouri, *Rev. Sci. Instrum.*, **86**, 0249031 (2015).

[18] J. W. Pomeroy, M. J. Uren, B. Lambert, and M. Kuball, *Microelectron. Reliab.*, **(55)12**, 2505 (2015).

ACRONYMS

AlGaN: Aluminium Gallium Nitride
CW: Continuous Wave
DGA: Direction Generale de l'Armement
DSTL: Defence Science and Technology Laboratory
EPSRC: Engineering and Physical Sciences Research Council
E2coGaN: Energy Efficient Converters using GaN Power Devices project
FE: Finite Element
GaN: Gallium Nitride
HEMT: High Electron Mobility Transistor
MCM ITP: Materials and Components for Missiles, Innovation and Technology Partnership
RF: Radio Frequency
SiC: Silicon Carbide